ACS OMEGA

Article

Cite This: ACS Omega 2018, 3, 7971−7978

Kinetically Doped Silica Sol−Gel Optical Biosensors: Expanding Potential Through Dip-Coating

Matthew S. Crosley and Wai Tak Yip*

Department of Chemistry and Biochemistry, University of Oklahoma, 101 Stephenson Parkway, Norman, Oklahoma 73071, United States

ABSTRACT: Kinetic doping has previously been shown to be an effective method of doping silica sol−gel thin films with an enzyme to construct biosensors. Until now, kinetic doping has only been applied to films produced through the spin-coating method. In this study, we present the use of dip-coating to produce thin films kinetically doped for biosensor development. In this way, kinetically doped biosensors may benefit from the increased range of substrate material shapes and sizes that may be easily coated through dip-coating but not spin-coating. The biosensors produced through dip-coating continue to show enhanced performance over more conventional enzyme loading methods with horseradish peroxidase and cytochrome C samples, showing an increase of 2400× and 1300× in enzyme concentration over that in their loading solutions, respectively. These correspond to enzyme concentrations of 5.37 and 10.57 mmol/L all while preserving a modest catalytic activity for the detection of hydrogen peroxide by horseradish peroxidase. This leads to a 77% and 88% increase in the total amount of horseradish peroxidase and cytochrome C, respectively, over that from coating the same glass coverslip via spin-coating methods.

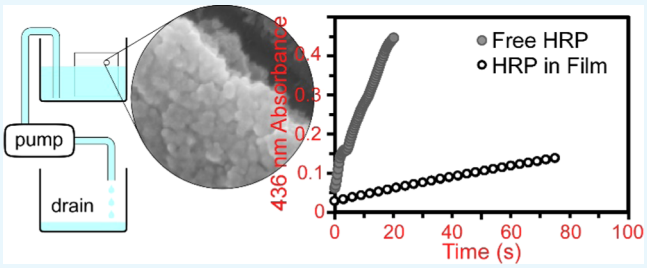

INTRODUCTION

Developing and improving biosensors based on immobilized enzymes continue to be an ongoing research effort garnering much attention. Immobilized enzymes display several considerable improvements compared with enzymes in solution, including, but not limited to, their reusability and relative ease of separation from any products produced. However, the challenge lies in both stably immobilizing the enzyme and preserving its activity that allow the resultant composite material to function as a biosensor. Ever since the first reported attempt to encapsulate protein within silica glass,[1] sol−gels have become a much investigated contender for use as an immobilization matrix.[2−12] With this increased attention, it has been well established that sol−gels do in fact meet these criteria as well as often improving the chemical and thermal stabilities of entrapped enzymes.[13] The convenience of being able to prepare thin films from sol−gel chemistry has even further enhanced its desirability as supportive matrix materials for biosensor development.[8]

Recently, our group has reported a new technique, known as kinetic doping,[14] to produce thin films highly loaded with the horseradish peroxidase (HRP) or cytochrome C (CytC) proteins via spin-coating.[15] As opposed to the established techniques,[16−18] pre-doping where a guest molecule is included with the sol solution and post-doping where any guest molecule is adsorbed to the surface-accessible areas of the film after the sol−gel chemistry for thin film formation has completed, often after heat annealing, kinetic doping takes advantage of a window of opportunity after casting the film and driving off the vast majority of the ethanol, but before the sol−gel chemistry on the film has progressed to a significant degree. The quick immersion in an aqueous loading solution significantly slows the poly-condensation step of the sol−gel process, extending the window for dopant loading before the film is fully set. If stayed immersed, it usually takes a week for a film to become fully set.

Kinetic doping produces films with an enhanced loading efficiency, whereas a comparable efficiency via pre-doping will require an exceedingly high dopant concentration in the sol solution that renders pre-doping almost impractical; this is especially true for the loading of expensive biomolecules. In the case of post-doping, a fully set film used in post-doping usually lacks big diffusion channels and dopant-accessible surfaces that are prerequisites for high loading efficiency. Kinetic doping allows dopant loading while diffusion channels and nascent solution-accessible surfaces are forming as the poly-condensation reaction slowly progresses, which appears to solve the problem of post-doping and demonstrated drastic loading capacity improvement over the more conventional method of post-doping. In particular, the sensor so produced exhibits a near-instantaneous response time that compared quite favorably to other modern systems, such as the chemiluminescence biosensor developed by Wang et al. that clearly shows a moderate delay in response time.[19]

One of the most favorable aspects of kinetic doping is its ability to accomplishing protein loading under a much more

Received: May 3, 2018
Accepted: June 25, 2018
Published: July 17, 2018

DOI: 10.1021/acsomega.8b00897
ACS Omega 2018, 3, 7971−7978

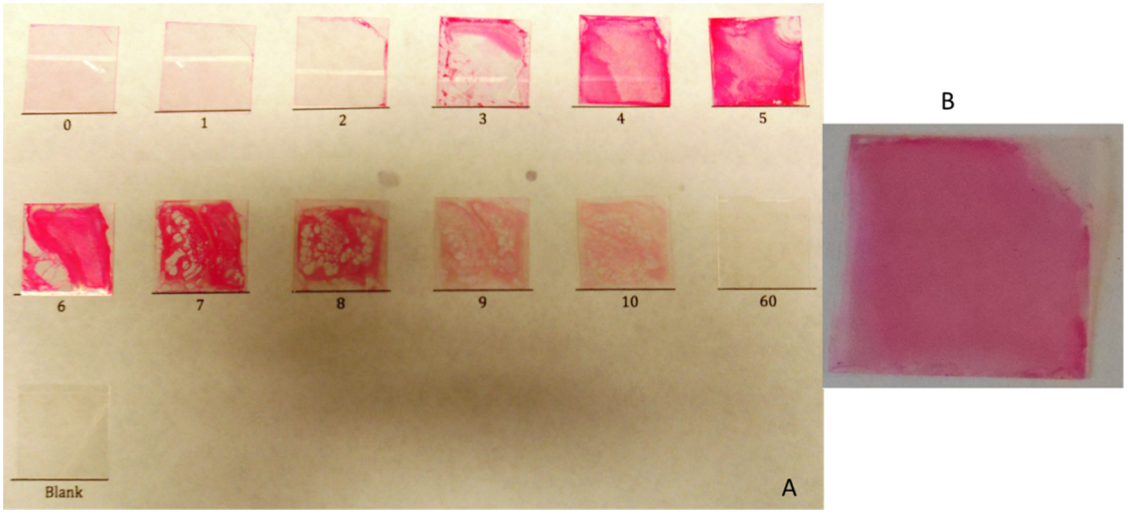

Figure 1. (A) Dip-coated thin films loaded with R6G arranged by time delay (in minutes) between coating and immersion in a R6G loading solution. (B) Improved film quality obtained under optimal delay time with better vibration control procedure.

benign environment without significantly affecting the sol−gel process. Because the most basic sol−gel casting procedure involves using a liquid sol mixture that usually has a sizeable composition in alcohol, it is quite natural that most enzymes will denature if they are introduced prior to the spin-coating process like pre-doping. Although a number of methods of circumventing this have been developed over the years, some involve the addition of stabilizers such as organosilanes or polyethylene glycol, whereas others take extra steps to produce a hybrid gel from modified precursors;[20] with most approaches inevitably increasing the material and labor cost for dopant loading. Kinetic doping is able to provide results of the same or even improved quality without the need for extra materials or laborious procedures, offering a significant advantage in both practical applications and cost effectiveness for commercialization.

In this work, we extend the kinetic doping technique to thin films produced by the dip-coating method. The previously utilized method of spin-coating has severe limitations on the size and shape of the substrates that can be coated. The high rotation velocity and the vacuum hold on the underside of the substrate to be coated limit spin-coating to small flat substrate platforms and only on one side of the substrate. Through dip-coating, where a thin film is formed via the removal of a substrate surface from a solution at a controlled speed, a wider range of material types, sizes, and shapes, including non-flat surfaces as well as surfaces on all sides of the substrate simultaneously, can be used to prepare kinetically doped enzyme-loaded thin films. Dip-coating techniques can be easily scaled to include larger and less conventional surfaces than spin-coating such that high dopant loading silica sol−gel thin film potential can dramatically be expanded to other practical uses. Here, we will report the process used to produce dip-coated thin films optimal for the loading of horseradish peroxidase and cytochrome C via kinetic doping and compare the catalytic performance of the biocomposite thin films with those prepared by spin-coating we reported previously.

RESULTS AND DISCUSSION

Loading of Rhodamine 6G (R6G). As has been shown with kinetically doped thin film samples produced via spin-coating, the delay time between the end of the coating process and the immersion in the soaking solution must be timed correctly to produce optimal loading results.[14] Figure 1A above displays the resulting rhodamine 6G-loaded thin films produced via dip-coating at various delay times ranging from no delay to a 10 min delay. It can be seen that a delay of between 0 and 3 min is not enough for the film to gain sufficient mechanical strength. The resultant samples suggest that the film might be thinning due to hydrolysis of the nascent film surface or the film could have fell apart and separated from the glass coverslip surface when introduced to the loading solution, leaving only the outermost edges of the film to remain attached. The same figure also suggests that a time delay of approximately 5−6 min appears to be the most appropriate delay for the film to properly adhere to the glass coverslip and yet pristine enough to enable kinetic doping. Any time delays longer than 5 min show the gradual passing of the window of opportunity for kinetic doping and led to a steady decline of the R6G loading capacity. At a delay of 60 min, the loading of R6G to the dip-coated film became negligible, as reflected by the apparently colorless 60 min sample, which is quite similar to the observation from spin-coated thin films and is likely caused by the film advancing along the poly-condensation process enough that the window for kinetic doping is closed and the process becomes far more similar to simple post-doping. On the basis of this observation, a 5 min delay was chosen for all subsequent studies on CtyC- and HRP-loaded thin films. The unevenness of the coating even at the optimal time delays demonstrates the need for a vibration-free environment after the coating. Even small vibrations appear to play a role in causing the sol to collect along the edges of the glass coverslip artificially thickening the film there. However, even in a completely vibration-free environment, the dip-coating process is known to have issues with edge effects, resulting in inhomogeneous areas extending slightly inward from the edges.[21] Subsequent experiments employing more stringent procedures that significantly suppress the vibration were able to produce more evenly loaded thin films such as the film shown in Figure 1B. Compared to that for spin-coating, where the optimal time delay is near zero,[15] the optimal time delay for dip-coating is longer. This can be explained as in spin-coating with its lengthy 70 s spinning process as well as approximately 30 more seconds for the spin coater to slow to a

DOI: 10.1021/acsomega.8b00897
ACS Omega 2018, 3, 7971−7978

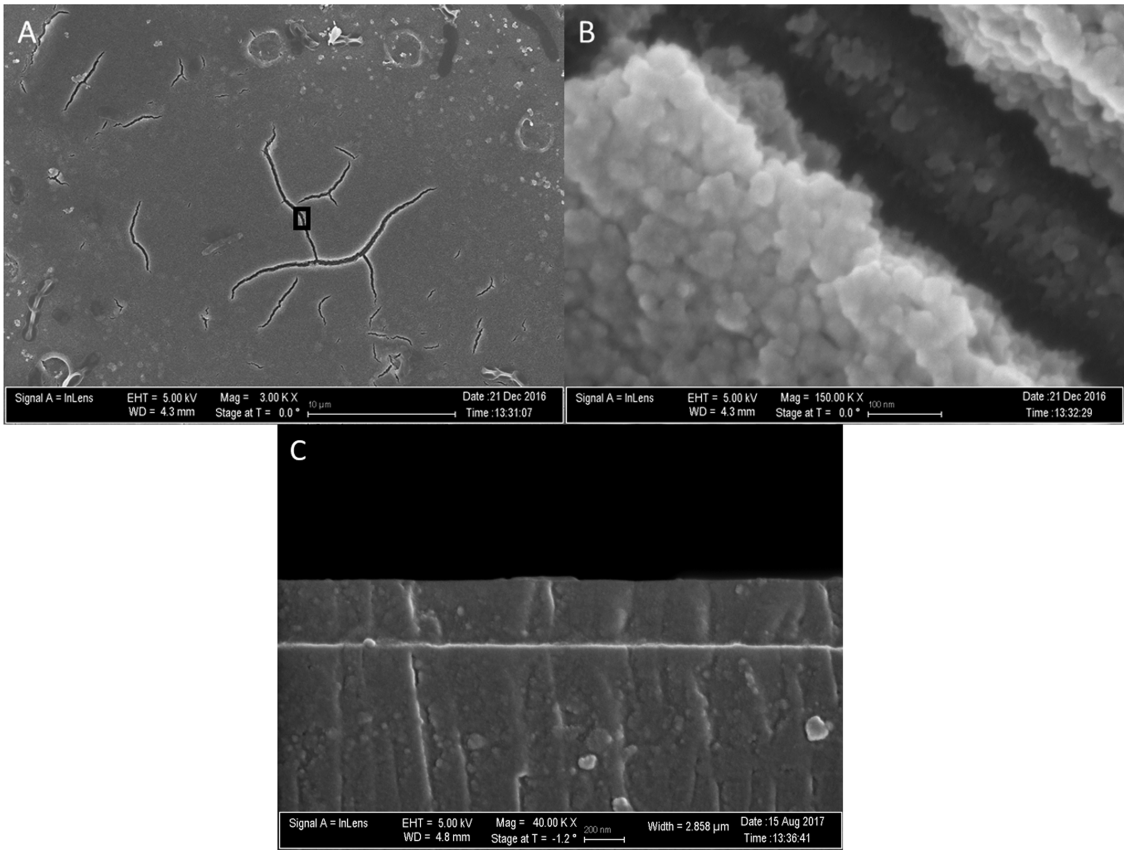

Figure 2. (A) SEM Image of a dip-coated thin film surface. (B) Enlarged view of the small area inside the black box shown in (A). (C) Thickness of a dip-coated film at the edge of a coverslip.

complete halt, which followed by another 10 s to dislodge the thin-film-coated coverslip from the vacuum hold before transferring to the loading solution, the time between the glass coverslip coming into contact with the sol solution and when it is available to be immersed in the loading solution in spin-coating is greater than the time needed for the dip-coating process. This, along with the high-speed rotation in spin-coating driving off ethanol faster than the stationary drain coating, likely leads to the spin-coated thin film being further along the film formation process than the dip-coated thin film meaning a longer delay time is required before the dip-coated film is in the optimal condition for immersion in the loading solution.

Scanning electron microscopy (SEM) images were obtained via JEOL JSM-880 with a 5 nm Au−Pd sputter-coated layer to examine the morphology of the dip-coated thin film produced using the 5 min delay determined for optimal kinetic doping. Figure 2A shows an average section of the thin film surface, which displays the presence of microscopic cracks on the silica film due to the shrinkage of the silica matrix caused by rapid drying induced by the vacuum used in the sputtering process. These random cracks, typically of any thin film sol−gel process,[1,2,4,6,8,12] are small enough that they do not significantly affect the mechanical strength of the silica film and cause the film to detach from the glass substrate, nor do they significantly reduce the area of the glass substrate covered by the thin film. Figure 2B shows the internal structure of a large crack displayed in Figure 2A and showcases the three-dimensional structure of the completely dip-coated thin film. Figure 2C shows the thin film from the edge and displays the interface between the thin film and the glass substrate as well as the thickness of the thin film coating. Flow control methods needed to ensure a 190 nm thickness were not applicable to the specially sized and cut sample shown side-on in Figure 2C, resulting in a slightly thicker than typical sample.

Loading of CytC and HRP. The quantification of loaded horseradish peroxidase and cytochrome C was carried out in a similar manner as previously used for quantifying loaded thin films[15] prepared from the spin-coating method. The calibration curve in Figure 3 shows a decrease in the 465 nm peak of Coomassie Brilliant Blue upon the step-wise addition of known

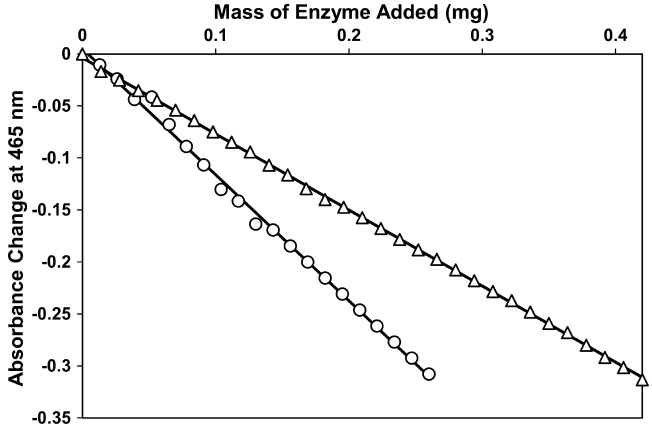

Figure 3. Calibration curves for cytochrome C (open circle) and horseradish peroxidase (open triangle) generated via an adapted Bradford assay against known enzyme concentrations.

DOI: 10.1021/acsomega.8b00897
ACS Omega 2018, 3, 7971−7978

amounts of enzyme and indicates a reasonably long linear range from which the mass equivalent of thin-film-loaded proteins can be estimated.

The experimental design used is such that the sol−gel film with the loaded protein on a glass coverslip substrate is placed on one side of a 45 mm(H) × 10 mm(D) × 40 mm(W) cuvette to prevent it from blocking the optical path of the UV−vis spectrometer and interfering with the measurement. After performing the Bradford assay on the protein-loaded thin films, the average change in absorbance determined from four replicate runs, such as the sample run shown for loaded HRP in Figure 4, was 0.037 ± 0.005 for CytC and 0.052 ± 0.009 for HRP.

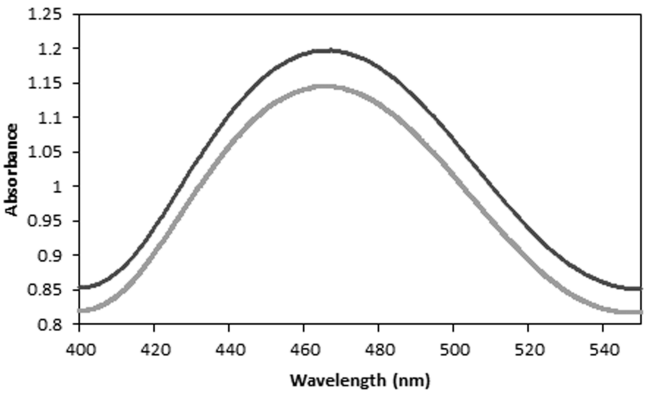

Figure 4. Completed Bradford assay for the loaded HRP thin film (gray line) compared with the original Bradford assay solution (black line).

From the calibration curve, the recorded absorbance decrease corresponds to 0.030 ± 0.005 mg of solution-accessible CytC and 0.055 ± 0.009 mg of solution-accessible HRP in a single thin film. This shows that the thin film had loaded 3.04% of CytC and 5.52% of HRP present in its enzyme loading solution. When taking into account the calculated thickness of the thin film based on the drain rate during dip-coating (190 nm), the coverslip surface area of 25 mm × 25 mm, which is then doubled to account for dip-coated thin films present on both sides of the glass coverslip, and the uncoated area of the glass coverslip that is held above the sol solution, 12.25 square mm, the volume of the thin film can be calculated, which can then be used to determine the concentration of solution-accessible protein in the thin film as 10.57 ± 1 mmol/L for CytC and 5.37 ± 0.5 mmol/L for HRP, approximately a 1300× and 2400× increase in concentration for CytC and HRP, respectively, compared to that of the original loading solutions of 0.1 mg/mL. Similar to the case of loading on spin-coated thin films, it is worth noting that these values take into consideration only the amount of dye-accessible protein as any protein inaccessible to the Coomassie Blue dye in the short time frame of the Bradford assay would not be accounted for by the assay. Because of the relatively large size of Coomassie Blue ($C_{47}H_{48}N_3NaO_7S_2$, FW: 854.02 g/mol), it is unlikely to diffuse through the porous thin film structure efficiently, meaning that it is quite possible that the actual amount of protein in the thin film is greater than what is being revealed by the Bradford assay.

The amounts of CytC and HRP loaded into the dip-coated films are summarized in Table 1 along with reference values obtained from loaded samples made through spin-coating[15] as well as a post-doped spin-coated sample and a blank coverslip control. Although the average change in absorbance for the dip-coated samples is nearly double that of the spin-coated sample, this is primarily due to the fact that the dip-coated method can produce thin films on both sides of the glass coverslip. The final enzyme concentration in one thin film after taking this difference into consideration provides a better metric for comparison. As an important advantage over spin-coating, the ability to coat both surfaces of the glass coverslip increased the total amount of enzyme loaded by 77% for the HRP thin film and 88% for the CytC thin film. It can be seen that both the HRP- and CytC-loaded thin films produced via dip-coating are very close in enzyme concentration to their spin-coated counterparts with only a slight decrease. On the other hand, it should also be noted that the dip-coated sample has a larger variation in enzyme loading efficiency than the spin-coated samples. This is currently thought to be caused by a larger variance in the film thickness caused by the dip-coating process compared to that by the spin-coating process, especially at the edge of the glass coverslip substrate. Further optimization of the dip-coating process, such as by using a commercially available dip-coater, is expected to minimize this thickness variation.

Just as with the spin-coated samples, the loading capacity accomplished by kinetic doping on dip-coated films represents a significant increase relative to that of the bare glass coverslip control sample. Without a porous film to immobilize the protein, the control sample showed only a marginal decrease in 465 nm absorbance in an identical Bradford assay. In fact, the magnitude of the absorbance change caused by the control samples was smaller than the error associated with the measurement. Also, just as the spin-coated samples, the dip-coated samples showed a great increase in loading capacity compared to that of the more conventional post-doping

Table 1. Loading Results

sample	average ΔA	average enzyme loading (mg)	conc. of soaking solution (mmol/L)	percent of soaking dopant loaded (%)	enzyme concentration in thin film (mmol/L)	increase over soaking solution
HRP	0.052 ± 0.009	0.055 ± 0.009	0.0023	5.52	5.37 ± 0.5	2400×
CytC	0.037 ± 0.005	0.030 ± 0.005	0.0082	3.04	10.57 ± 1	1300×
HRP from spin-coating	0.023 ± 0.004	0.031 ± 0.002	0.0023	3.09	6.0 ± 0.4	2600×
CytC from spin-coating	0.020 ± 0.002	0.016 ± 0.002	0.0082	1.57	11 ± 1	1300×
bare coverglass	0.001 ± 0.002	0.001 ± 0.002	0.0082	0.08		
post-doped HRP control	0.005 ± 0.003	0.005 ± 0.003	0.0023	0.5	1.0 ± 0.6	430×

DOI: 10.1021/acsomega.8b00897
ACS Omega 2018, 3, 7971−7978

method that reached only 18.6% of the enzyme concentration prepared from kinetic doping.

Quantification of HRP Activity. Following the determination of the enzyme concentration loaded in the dip-coated thin films, the next vital aspect of function for a biosensor is the retention of catalytic activity. The activity of HRP-loaded thin films created via dip-coating was measured in the same manner as the thin films created via spin-coating. An assay solution that contains 140 μM H_2O_2 and 300 μM guaiacol was used, where a distinctive brown quinone, believed to be mostly from a dimeric product, forms by the catalytic action of thin-film-encapsulated HRP. The products produced at the film surface would gradually diffuse into the bulk assay solution, and the rate of production of the product could be conveniently monitored by UV−vis spectroscopy at 436 nm in real time. The activity was determined using the initial rate method by examining the initial increase of the linear portion of the 436 nm absorbance trace for both the free HRP and the thin-film-immobilized HRP as a function of reaction time shown in Figure 5 below.

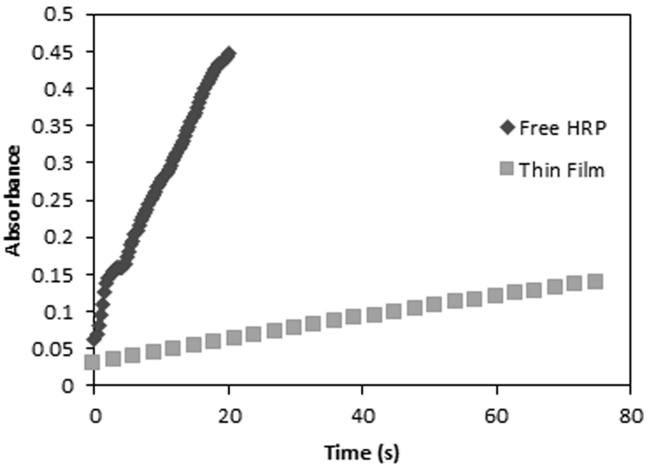

Figure 5. Activity of free HRP and the HRP-loaded thin film.

The activity per mg HRP can be calculated from the rate of guaiacol consumption via eq 1

$$\frac{\Delta A_{436\ \mathrm{nm}} \times 2V_t}{t_{\mathrm{minutes}} \times \varepsilon \times M} \quad (1)$$

where V_t is the total assay solution volume, ε is the extinction coefficient of the brown quinone dimer at 436 nm, M is the mass of HRP present (in mg), and 2 is a constant related to the stoichiometric ratio of guaiacol to its dimeric product per reaction. Table 2 gives the resulting activity values for the HRP-loaded thin film via dip-coating as well as the reference values for free HRP and HRP loaded in spin-coated thin films.

The data show that HRP exhibits a decrease in activity when immobilized in a solid matrix, as expected for all such entrapped enzymes. The activity (U/mg) of HRP in a dip-coated thin film is slightly less than in a spin-coated thin film, but still within the range of error, resulting in a similar activity per mg loading, as seen in Table 2. As with the spin-coated thin films, the drop in activity relative to free HRP is thought to be due to the limited rates of diffusion through the film's dense three-dimensional network. Furthermore, this is likely exacerbated by the increase in size from the guaiacol as it transforms into its larger dimeric product, 3,3′-dimethoxy-4,4′-biphenoquinone ($C_{14}H_{12}O_4$, FW: 244.25 g/mol). It is important to note that the brown dimeric guaiacol product from the catalyzed reaction can be seen to be formed on the surface of the thin film almost instantly upon immersion in the reaction solution. This is well before the brown color of the product can be seen to be mixed with the rest of the reaction assay solution, serving as further evidence that it is the outward diffusion of the larger product that is the primary limiting factor to the rate of the catalytic reaction.

Table 2. Activity Results

sample	activity (U/mg)	% of free HRP
free HRP	35.4 ± 0.8	100
spin-coated thin film	4.1 ± 0.2	11.7 ± 0.5
dip-coated thin film	3.7 ± 0.2	9.7 ± 0.5

The observed drop in activity is not totally unexpected as the earliest examples of enzymes encapsulated in sol−gels were able to display only a little more than 1% of their activity.[22−24] As the field continued to advance such that longer and more involved processes are developed to produce the latest HRP/sol−gel biocomposite material, a retention reaching 10% of the original activity was observed from a similar guaiacol assay.[25] We observe very nearly the same result using the much simple kinetic doping process reported here.

Previously, one of the highest concentrations of HRP attained in a silica sol−gel structure was achieved by Bhatia and Brinker, producing silica sol−gel monoliths of up to 1 mM.[24] The results reported in this study not only represent a much higher enzyme concentration but also are produced via a much simpler technique and is applied as a thin film coating technique, a far more advantageous and versatile platform than the powder produced from a monolith.

CONCLUSIONS

In this study, the first application of the dip-coating technique was implemented to kinetic doping to produce active biocomposite thin films. HRP- and CytC-loaded films were produced and tested. Our results indicate that merging dip-coating and kinetic doping together proved to be a promising approach to biosensor development, trapping larger quantities of the loaded enzymes than those obtained in most conventional methods, increasing the amount of enzyme loaded by 77% and 88% over the same piece of substrate material coated with the spin-coating technique, while retaining activity that approaches 10% of an equivalent amount of free HRP. With high loading capacity and moderate retention in activity on the same level as that in the previously established spin-coating methods, dip-coating certainly represents an even more attractive approach as it effectively expands the enzyme-loaded thin film coating to a much wider range of material shapes and sizes to be used in conjunction with a much simple yet protein friendly process of kinetic doping that is most compatible for biosensor fabrication. The ability to easily scale up dip-coating processes to handle larger substrate sizes and its ability to coat all available surfaces at once give dip-coating a considerable edge in versatility over spin-coating.

EXPERIMENTAL SECTION

Materials and General Methods. Tetraethylorthosilicate (TEOS), CytC (from equine heart), 2, 2′-azino-bis(3-ethyl-

DOI: 10.1021/acsomega.8b00897
ACS Omega 2018, 3, 7971−7978

benzothiazoline-6-sulfonic acid) diammonium salt (ABTS), and Coomassie Brilliant Blue G-250 were purchased from Sigma-Aldrich. Phosphoric acid and hydrogen peroxide (30% solution) were purchased from EMD Millipore. HRP was purchased from Gold Biotechnology. Guaiacol was purchased from Cayman Chemical Company. Premium grade glass coverslips (25 mm × 25 mm × 1 mm) were purchased from Fisher Scientific. All chemicals and materials were used as received, with the exception of the glass coverslips, which were cleaned prior to use. All UV−vis spectra were obtained via a Shimadzu UV-2101PC UV−vis spectrometer.

Preparation of Glass Coverslips. To remove any organic contaminants on the glass coverslip surface, the coverslips were sonicated in an acetone bath for 30 min and rinsed with Millipore water three times to remove all acetone. The organic contaminant-free coverslips were then sonicated in 10% v/v NaOH for another 30 min and rinsed with Millipore water three times to remove all residual NaOH. The coverslips then went through a final sonication in Millipore water for 30 min to remove all traces of NaOH. Afterward, the coverslips were stored in Millipore water until use.

Preparation of Silica Sol. Silica sol was prepared by mixing 56.0 mL of TEOS, 111.7 mL of ethanol, 31.7 mL of Millipore water, and 0.620 mL of a 1% v/v phosphoric acid solution at room temperature. The sol was allowed to age for 18 h at room temperature in the dark before use.

Preparation of Rhodamine 6G and CytC- and HRP-Doped Silica Sol−Gel Thin Films. Instead of using the conventional dip-coating approach, the dip-coated thin film was prepared by draining a coating sol solution from a beaker. After aging for 18 h, the silica sol solution was transferred to a 400 mL beaker that is elevated by a jack stand. A clean coverslip was purged, dried via compressed air, and suspended from above while it was immersed in the aged silica sol coating solution. The sol solution was drained from the beaker with a pump at a known flow rate intended to result in a thin film coating thickness comparable to that of the 190 nm thick samples previously produced and studied via the spin-coating methods.[15] The required flow rate to produce the 190 nm thick films was calculated via the Landau−Levich equation.[26]

Immediately following the complete drainage of the silica sol solution, the jack stand holding the beaker was lowered until the newly coated coverslip was completely outside of the beaker and exposed to ambient air. The newly made thin film was allowed to remain exposed in ambient air for another 5 min before it was transferred to a loading solution, where R6G, CytC, or HRP will be loaded into the silica film via kinetic doping. R6G loading solutions consisted of 10 mM R6G in a pH 7.4 phosphate buffered saline (PBS) buffer, while enzyme loading solutions consisted of 0.1 mg/mL enzyme suspended in a 10 mM, pH 7.4 PBS buffer.

A total of three different kinds of control samples were prepared. (i) Control samples of enzyme loaded on bare glass were prepared by placing a freshly cleaned glass coverslip directly into the CytC or HRP loading solutions that also consisted of 0.1 mg/mL enzyme suspended in a 10 mM pH 7.4 PBS buffer for the same period of time as that for the sample thin films; (ii) control samples of thin films with no enzyme loading were prepared by soaking a sol−gel film in a 10 mM, pH 7.4 PBS buffer that contains no enzyme with an immersion time same as that for the sample films; (iii) post-doped controls were prepared by allowing the nascent thin-film-coated coverslips to age for 48 h, allowing the film to fully set under ambient temperature before submersion in the CytC or HRP loading solution.

Quantitative Determination of Cytochrome C and Horseradish Peroxidase Loading. The mass of the loaded protein was quantified via a modified Bradford assay using a standard calibration curve. The assay solution was prepared according to the original Bradford method.[27] Namely, 100 mg of Coomassie Brilliant Blue dye G-250 is dissolved in 50 mL of ethanol and the reaction mixture is then added to 100 mL of concentrated phosphoric acid and diluted to 1 L with deionized water. Upon binding to an enzyme like CytC and HRP, the absorption maxima of the dye will exhibit a significant red shift from 465 to 595 nm. This 130 nm red shift is large enough that the disappearance of the 465 nm peak can be reliably used to measure the removal of free dye upon binding to the thin-film-immobilized enzyme, with very little influence from the emerging 595 nm peak.

To quantify the amount of enzyme loading, the enzyme-loaded thin film samples were submerged in 10 mL of the Bradford assay solution inside a 45 mm(H) × 10 mm(D) × 40 mm(W) cuvette that was continuously stirred. This extra wide cuvette not only allows the entire coverslip to be placed inside but also provides enough space to ensure that the enzyme-loaded coverslip is not in the optical path of the UV−vis spectrometer, preventing any interference from the coverslip itself or from any dye bound to the enzyme-loaded coverslip during the real-time absorption measurements. The Coomassie Blue dye would bind to solution-accessible enzymes that were loaded inside the thin film, thereby lowering the concentration of free dye in the assay solution. By monitoring the depletion of free dye absorption at 465 nm, the quantity of loaded enzyme that is accessible to free dyes could be determined. The reduction in 465 nm absorbance was recorded and then compared with a calibration curve obtained from a separate Bradford assay using a series of known concentrations of CytC and HRP from the same stock. This was accomplished by recording the decrease in 465 nm absorbance while a fixed amount of enzyme was added to a Bradford assay solution in a step-wise fashion.

Detection of Cytochrome C in Loaded Thin Films. After 1 week of kinetic doping in a CytC loading solution, thin film samples were removed and washed under a direct stream of running distilled water to remove all CytC that is loosely bound to the thin film surface. The presence of active CytC in the thin film was determined through an ABTS solution assay. In this assay, ABTS was chosen due to its easily observable color change (from colorless to green), ease of storage and preparation, and a good body of existing literature about its catalytic transformation by CytC in the presence of H_2O_2. The clear ABTS assay solution was prepared by adding 14 μL of 30% H_2O_2 to 100 mL of a 14 μM ABTS solution made with a 10 mM, pH 7.4 PBS buffer. The resultant H_2O_2 concentration in the assay solution was 1.4 mM. The assay was performed by directly submerging the CytC-loaded thin film in the ABTS assay solution. The presence of active CytC in the silica film could be observed visually from the appearance of green products on the surface of the coverslip, with the green products slowly diffusing into the once colorless assay solution.

Detection of Horseradish Peroxidase in Loaded Thin Films. Similar to the CytC-loaded thin films, the HRP-loaded coverslips were removed after 1 week of kinetic doping in a HRP loading solution, which were then washed with distilled water to remove loosely bound enzymes. The presence of thin-

DOI: 10.1021/acsomega.8b00897
ACS Omega 2018, 3, 7971−7978

film-loaded HRP was verified by a guaiacol solution assay. Guaiacol was chosen for the assay because of the dramatic color change from colorless to dark brown as it was catalytically oxidized into the dimeric and tetrameric quinone products by HRP in the presence of H_2O_2. The color change is easily observable even to the naked eye. The guaiacol assay solution is a mixture of 1.4 μL of 30% H_2O_2 and 3.3 μL of liquid guaiacol in 100 mL of a 10 mM, pH 7.4 PBS buffer. The resultant H_2O_2 and guaiacol concentrations in the assay solution are 140 and 300 μM, respectively. To prevent the inactivation of HRP by excess H_2O_2, low H_2O_2 concentration was deliberately used in the design of this assay. In this assay, the stoichiometric ratio between H_2O_2 and guaiacol was kept slightly below 1.0 to favor catalytic dimer formation. The assay was carried out by directly submerging the HRP-loaded thin film into the clear guaiacol assay solution. Subsequently, the presence of active HRP could be visually confirmed by the formation of brown quinone products on the thin film surface, which then gradually diffuse outward and spread through the once colorless assay solution.

Quantification of HRP Catalytic Activity. The catalytic activity of thin-film-immobilized HRP was determined by following the rate of product formation in a HRP/guaiacol assay reaction. The reaction was monitored in real time via the increase in the quinone product absorption at 436 nm under continuous stirring. To compare the activity of free and thin-film-bound HRP, the same experiment was repeated for the same quantity of both free HRP and HRP loaded in a thin film. The activity of HRP was calculated from the initial rate method that utilizes the linear portion of the 436 nm absorbance time course captured.

AUTHOR INFORMATION

Corresponding Author

*E-mail: ivan-yip@ou.edu.

ORCID

Matthew S. Crosley: 0000-0001-8217-5653

Author Contributions

The manuscript was written through contributions of all authors. All authors have given approval to the final version of the manuscript.

Notes

The authors declare no competing financial interest.

ACKNOWLEDGMENTS

This work was supported by Oklahoma Centre for the Advancement of Science and Technology (HR 12-128).

REFERENCES

(1) Braun, S.; Rappoport, S.; Zusman, R.; Avnir, D.; Ottolenghi, M. Biochemically active sol-gel glasses: the trapping of enzymes. *Mater. Lett.* **1990**, *10*, 1−5.

(2) Jin, W.; Brennan, J. D. Properties and applications of proteins encapsulated within sol-gel derived materials. *Anal. Chem. Acta* **2002**, *461*, 1−36.

(3) Avnir, D.; Coradin, T.; Lev, O.; Livage, J. Recent bio-applications of sol-gel materials. *J. Mater. Chem.* **2006**, *16*, 1013−1030.

(4) Kato, M.; Shoda, N.; Yamamoto, T.; Shiratori, R.; Toyooka, T. Development of a silica-based double-network hydrogel for high-throughput screening of encapsulated enzymes. *Analyst* **2009**, *134*, 577−581.

(5) Simon, D. N.; Czolk, R.; Ache, H. J. Doped sol-gel films for the development of optochemical ethanol sensors. *Thin Solid Films* **1995**, *260*, 107−110.

(6) Cerqua, K. A.; Hayden, J. E.; LaCourse, W. C. Stress measurements in sol-gel films. *J. Non-Cryst. Solids* **1988**, *100*, 471−478.

(7) Zusman, R.; Rottman, C.; Ottolenghi, M.; Avnir, D. Doped sol-gel glasses as chemical sensors. *J. Non-Cryst. Solids* **1990**, *122*, 107−109.

(8) Jerónimo, P. C. A.; Araujo, A. N.; Montenegro, C. B. S. M. Optical sensors and biosensors based on sol-gel films. *Talanta* **2007**, *72*, 13−27.

(9) Narang, U.; Prasad, P. N.; Bright, F. V.; Ramanathan, K.; Kumar, N. D.; Malhotra, B. D.; Kamalasanan, M. N.; Chandra, S. Glucose biosensor based on a sol-gel derived platform. *Anal. Chem.* **1994**, *66*, 3139−3144.

(10) Rottman, C.; Ottolenghi, M.; Zusman, R.; Levb, O.; Smith, M.; Gong, G.; Kagan, M. L.; Avnir, D. Doped sol-gel glasses as pH sensors. *Mater. Lett.* **1992**, *13*, 293−298.

(11) Rottman, C.; Turniansky, A.; Avnir, D. Sol-Gel physical and covalent entrapment of three methyl red indicators: a comparative study. *J. Sol-Gel Sci. Technol.* **1998**, *13*, 17−25.

(12) Ciriminna, R.; Fidalgo, A.; Pandarus, V.; Béland, F.; Ilharco, L.; Pagliaro, M. The Sol-Gel Route to Advanced Silica-Based Materials and Recent Applications. *Chem. Rev.* **2013**, *113*, 6592−6620.

(13) Pierre, A. C. The sol-gel encapsulation of enzymes. *Biocatal. Biotransform.* **2004**, *22*, 145−170.

(14) Campbell, A. L. O.; Lei, Q.; Yip, W. T. Kinetic approach to hyper-doped optical quality thin films. *Chem. Commun.* **2014**, *50*, 9321−9324.

(15) Crosley, M. S.; Yip, W. T. Silica Sol-Gel Optical Biosensors: Ultrahigh Enzyme Loading Capacity on Thin Films via Kinetic Doping. *J. Phys. Chem. B* **2017**, *121*, 2121−2126.

(16) Calvo, A.; Joselvich, M.; Soler-Illia, G. J. A. A.; Williams, F. J. Chemical reactivity of aminofunctionalized mesoporous silica thin films obtained by co-condensation and postgrafting routes. *Microporous Mesoporous Mater.* **2009**, *121*, 67−72.

(17) Nicole, L.; Boissiere, C.; Grosso, D.; Quach, A.; Sanchez, C. Mesostructured hybrid organic-inorganic thin films. *J. Mater. Chem.* **2005**, *15*, 3598−3627.

(18) Mackenzie, J. D.; Huang, Q.; Iwamoto, T. Mechanical properties of ormosils. *J. Sol-Gel Sci. Technol.* **1996**, *7*, 151−161.

(19) Wang, K. M.; Li, J.; Yang, X.; Shen, F.; Wang, X. A chemiluminescent H2O2 sensor based on horseradish peroxidase immobilized by sol-gel method. *Sens. Actuators, B* **2000**, *65*, 239−240.

(20) Ronda, L.; Bruno, S.; Campanini, B.; Mozzarelli, A.; Abbruzzetti, S.; Viappiani, C.; Cupane, A.; Levantino, M.; Bettati, S. Immobilization of Proteins in Silica Gel: Biochemical and Biophysical Properties. *Curr. Org. Chem.* **2015**, *19*, 1653−1668.

(21) Arfsten, N. I.; Eberle, A.; Otto, J.; Reich, A. Investigations on the angle-dependent dip coating technique (ADDC) for the production of optical filters. *J. Sol-Gel Sci. Technol.* **1997**, *8*, 1099−1104.

(22) Bhatia, R. B.; Brinker, C. J.; Gupta, A. K.; Singh, A. K. Aqueous sol-gel process for protein encapsulation. *Chem. Mater.* **2000**, *12*, 2434−2441.

(23) Badjić, J. D.; Kostic, N. M. Effects of Encapsulation in Sol-Gel Silica Glass on Esterase Activity, Conformational Stability, and Unfolding of Bovine Carbonic Anhydrase II. *Chem. Mater.* **1999**, *11*, 3671−3679.

(24) Sheltzer, S.; Rapporport, S.; Avnir, D.; Ottolenghi, M.; Braun, S. Properties of trypsin and of acid phosphatase immobilized in sol-gel glass matrices. *Biotechnol. Appl. Biochem.* **1992**, *15*, 227−235.

(25) Smith, K.; Silvernail, N. J.; Rodgers, K. R.; Elgren, T. E.; Castro, M.; Parker, R. M. Sol-Gel Encapsulated Horseradish Peroxidase: A Catalytic Material for Peroxidation. *J. Am. Chem. Soc.* **2002**, *124*, 4247−4252.

(26) Landau, L.; Levich, V. Dragging of a Liquid by a Moving Plate. *Acta Physicochim. URSS* **1942**, *17*, 42−54.

DOI: 10.1021/acsomega.8b00897
ACS Omega 2018, 3, 7971−7978

(27) Bradford, M. M. A rapid and sensitive method for the quantitation of microgram quantities of protein utilizing the principle of protein-dye binding. *Anal. Biochem.* **1976**, *72*, 248−254.

DOI: 10.1021/acsomega.8b00897
ACS Omega 2018, 3, 7971−7978